Turkish Journal of Electrical Engineering & Computer Sciences

http://journals.tubitak.gov.tr/elektrik/

Research Article

Turk J Elec Eng & Comp Sci
(2017) 25: 4457 – 4473

doi:10.3906/elk-1612-167

A novel and realistic hybrid downlink-uplink coupled/decoupled access scheme for 5G HetNets

Nadeem SIAL*, Junaid AHMED
COMSATS Institute of Information Technology, Islamabad, Pakistan

Received: 14.12.2016 • **Accepted/Published Online:** 21.09.2017 • **Final Version:** 03.12.2017

Abstract: Cell association in present day heterogeneous networks (HetNets) is still based on the technique used by homogeneous cellular networks despite power and coverage area disparities of network nodes. In ongoing policy, both uplink (UL) and downlink (DL) associations are coupled based on DL characteristics, which introduces UL-DL asymmetry and cell load imbalances. Recently, decoupled cell association, also known as downlink-uplink decoupling (DUDe), has been introduced in 3rd Generation Partnership Project (3GPP) Release 12 to improve uplink performance, load balancing, and cell capacity. In DUDe, characteristics of both DL and UL channels can be considered. By using this concept, various theoretical UL or DL analytical decoupled access models have been proposed without giving their practical realization. In these frameworks, all network users are assumed to use DL-UL decoupled access without considering its practical utility. Existing solutions also ignore noise, which may lead to practical inaccuracies. This paper proposes a novel and realistic hybrid scheme in which coupled or decoupled cell associations can be selected depending upon user location and its advantages. Building upon this innovative approach, it has been established that decoupled access is chosen by few users and accordingly a two-tier analysis framework for these devices has been formulated. Simple closed-form solutions for user performance metrics without ignoring noise have been precisely derived, which relate user performance with HetNet densities. Devised distributions are employed to compare the performance of the decoupled case with the ongoing procedure of coupled access. A practical network design has been proposed, which requires minimum changes to the existing network. Results show that decoupling is viable in the 5G HetNet to achieve fairness, cell load balancing, and performance improvements.

Key words: HetNet, 5G, decoupling, association probabilities, DUDe analysis

1. Introduction

Ever increasing data, mobility, and fairness demands of users have transformed conventional homogeneous cellular networks (HCN) into highly dense HetNets [1,2]. This heterogeneity is expected to be a key feature for improving network performance for forthcoming 5G networks [2–4]. In HetNets, low-power small cells, i.e. femto or pico, are deployed with high-power macrocells, which brings power and coverage area disparities among deployed nodes. In these networks, the downlink coverage areas of macrocells are much larger than those of low-power femto or pico cells due to differences in downlink transmit powers, antenna heights, and antenna gains, which bring coverage area asymmetries. However, cell association in present HetNets is still based on the old and less effective procedure used by HCNs. Presently, both DL and UL are linked to same base-station (BS) and this decision is based on downlink reference signal received power (DLRP) despite the differences of

*Correspondence: nadeem_606@yahoo.com

BS power and coverage areas. In the existing association policy, a user may be connected to a macrocell in uplink due to power disparities even though the path loss to a small cell is lower, resulting in low user uplink performance. Due to this type of inefficient cell association, small cells may be overloaded in DL while unloaded in UL, causing uneven load distribution between macrocells and small cells. Moreover, all users of macrocells do not get equal chances to equalize their performance metrics in existing cell associations. The cell edge users remain underprivileged and are unable to equalize their performances with other users located close to macrocells. In order to address these issues, the concept of downlink-uplink decoupling (DUDe) was introduced in 3rd Generation Partnership Project (3GPP) Release 12 [5]. In DUDe, UL and DL are decoupled and a user can connect with one BS in DL based on DLRP and another BS in UL based on path loss, providing the highest UL throughput [3–8]. This decoupling is viable because the performance of HetNets critically depends on their spatial configuration [3]. Moreover, this decoupling also achieves cell load balancing, fairness among users, and significant capacity gains to underprivileged cell edge users for executing online social, video chatting, and gaming applications. In the uplink, all transmitters have roughly the same maximum transmit power in HetNets. Hence, in decoupled access, a mobile that is associated to a macrocell in the downlink may be linked to a femto or pico cell in the uplink to take advantage of the reduced path loss. Therefore, connection to a closer small cell provides higher user performance and optimum capacity in the uplink, which in turn ensures fairness among users at the network level.

In this paper, we propose a new and practical hybrid coupled/decoupled cell association scheme that can be selected depending upon user location and by considering its benefits. Building upon this innovative approach, we have modeled a two-tier HetNet in which decoupled access has been permitted. This policy brings certain changes to network access and user types, as shown in Figure 1. Now one type of user can have UL-DL coupled association (CoA) with the same BS (macrocell, picocell, or femtocell) despite the permissibility of decoupled association. Such users can follow existing DLRP-based access without requiring any changes to their association process. A second type of user can follow the UL-DL decoupled access called DUDe association policy. In DUDe, the user DL can be associated with macrocells based on DLRP and UL with picocells or femtocells due to proximity or shorter distance. In order to conform to DUDe policy, it is necessary that the user be located at a place where UL-DL decoupling with two different cells is possible. From this setup, it can be established that decoupling primarily changes the access procedure of some of the network users and not all of them. Therefore, a tractable analytical model is required for users who meet the DUDe association policy. The remaining CoA users can continue following DLRP-based cell association as given in [4].

Our hybrid coupled/decoupled access approach completely differs from existing decoupled access methods [5–7,9]. In these prior works, various theoretical UL or DL analytical decoupled access models were proposed without giving their practical realization. In these frameworks, all network users are assumed to utilize decoupled access in UL or DL without considering its necessity and viability. Moreover, the existing analytical models also ignore noise, which can lead to practical scenario inaccuracies. Furthermore, they only focus on characterization of channels without providing insight on the decoupling effects in terms of degree of HetNet densities required to meet quality of service (QoS) objectives. In our work, we first classify the users according to location and type. Later on, we apply the decoupled access policy for those users who can take advantage of it. Based on this concept, we have derived a two-tier uplink analysis framework for network devices that are mainly affected by decoupling. Using this model, simple closed-form analytical solutions for the complementary cumulative distribution function (CCDF) of signal-to-interference plus noise ratio (SINR) and average throughput have been derived without ignoring noise. The results are accurate for stated performance metrics and mathematical

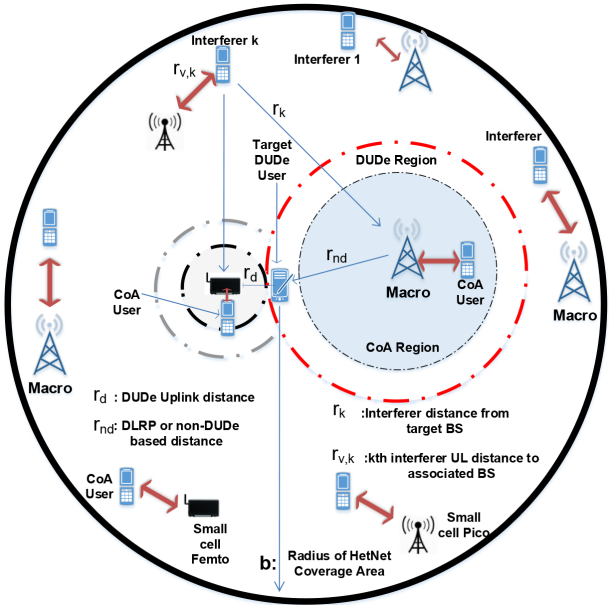

Figure 1. A typical HetNet scenario with decoupling.

model correctness has been certified by comparing the theoretical results with the simulation. For downlink association, the analytical model given in [4] can be used. Major contributions and outcomes of paper are:

- A hybrid coupled/decoupled association scheme for HetNets has been proposed, which is practical in nature. Based on this scheme, simple analytical closed-form expressions for decoupled users have been derived without ignoring noise to quantify decoupled access advantages. Moreover, contrary to existing research on HetNets, we have shown that analytical models without noise can give inaccurate results.
- Our derived distributions relate user performance to degree of HetNet densities and BS power for designing efficient networks meeting QoS objectives.
- Based on the conducted analysis, a practical network architecture for decoupled access has been proposed, which requires minimum changes to existing network design as opposed to solutions proposed in [6,7], where practical implications have been neglected.

The paper is organized as follows. Section 2 gives the system model, and in Section 3, we derive the CCDF of SINR for DUDe and non-DUDe. Section 4 gives average throughput analysis, Section 5 gives numerical results, Section 6 gives the practical decoupled network design, and Section 7 concludes the paper.

2. Uplink system model

We model a two-tier HetNet with macrocells and small cells (picocells or femtocells) as shown in Figure 1. In this HetNet, the decoupling of UL and DL has been analyzed by using stochastic geometry. For decoupled access, users are associated with a macrocell in downlink and a femtocell or picocell in uplink. Tiers of BSs are distinguished by their spatial densities and transmit powers. For analysis, all network users, interferers, macrocells, and small cells are supposed within a circular region having radius b (outermost circle with solid line as shown in Figure 1). The target user is assumed to be located at the center of a big circle. By Slivnyak's

theorem [10], the distribution of a point process in R^2 is unaffected by the addition of a node (target user) at the origin. Dotted circles around macrocells and small cells show the different types of association regions, i.e. CoA or DUDe. Inner dotted circles around each BS in Figure 1 show the hypothetical regions where CoA is chosen by users. The region between inner and outer dotted circles around each BS show the DUDe area where decoupled UL-DL association is more viable due to shorter distance from closely located femtocells or picocells. This decoupled region also provides the advantage of applying load balancing separately for UL-DL and it also facilitates optimal cell capacity in UL-DL. This decoupled region is bounded by $\frac{P_s}{P_m} r_d^{-\alpha} < r_{nd}^{-\alpha} \leq r_d^{-\alpha}$, where $\frac{P_s}{P_m} < 1$. The size of this region is fixed for particular cell densities, user locations, and settings of BS power levels (in existing HetNets, macrocells transmit at 46 dBm and small cells at 20 dBm). In the current long-term evolution (LTE) HetNet design, without the UL-DL decoupling, range extension called cell range extension (CRE) [4] is used to offset the DLRP of small cells and to balance the cell load. In CRE, a user is associated to a small cell instead of a macrocell by addition of a cell-specific offset (CSO) in DLRP. This creates a CRE region around the small cell whose size depends upon the selection of the CSO value. Currently, one of the main challenges in cell range extension for LTE has been to determine the optimal range extension bias or CSO value in dBs as users connected to a small cell with CRE may experience strong interference from the macrocell. To solve this, enhanced intercell interference coordination (eICIC) is recommended with CRE, which results in negative impact on the overall system capacity due to the reduction of schedulable subframes [4]. However, in the case of decoupled cell associations, there are no trade-offs like CSO selection in CRE and the size of the DUDe region remains constant for a particular HetNet environment.

In our system model, the locations of users, macrocells, femtocells, or picocells are modeled with independent homogeneous Poisson point processes (PPPs) as proposed in [4,7]. Let φ_v denote the set of points obtained through a PPP with density λ_v, where $v = m$ for macrocells and $v = s$ for femtocells or picocells. Let us suppose that users are also located according to homogeneous PPPs, φ_u with density λ_u. Currently, spectrum-sharing schemes for the 5G cellular network have not been defined and we assume that orthogonal frequency division multiple access (OFDMA) is being used, as also argued in [7]. Exactly one interfering user exists in each cell for the target user, whose performance metrics are being calculated and whose density of interfering users, λ_I, is $\lambda_I = \lambda_m + \lambda_s$. In OFDMA, interfering users are located outside the association region of the target BS. Due to an interferer with random location within its own BS coverage region, uplink interference can be viewed as stemming from a Voronoi perturbed lattice process whose functional form is not tractable [7]. In our model, we have used an inhomogeneous PPP to approximate the locations of interfering users. For this process, we have randomly chosen a user from each of the other BSs to define the point process consisting of the chosen users as φ_I, as recommended by Sui et al. [11]. The uplink desired and the interference signals experience path loss factor α, which is the same for both tiers due to the same wireless communication environment. However, path losses for uplink and downlink for DUDe users is different. As shown in Figure 1, let r_i be the distance of the target user from the serving BS in uplink, where $i = nd$ for the non-DUDe case or DLRP-based association and $i = d$ for DUDe. Let $h_{r_i v}$ be channel gain between the target user at distance r_i from vBS and h_{r_k} represents channel gain on the kth interferer located at distance r_k from the target user in UL. We have modeled channel gain as slow-flat Rayleigh faded. For log normal shadowing, we use the approach elaborated in [12], where the authors included shadowing in a transparent way by using the displacement theorem given in [13]. We have used fractional power control (FPC) in UL. In UL, all transmitters have roughly the same maximum transmit power with FPC to conserve energy and also to reduce interference [7,14,15]. Use of FPC is

also supported by 3GPP LTE networks to partially compensate for path losses [16]. In UL, DUDe area users, required to transmit at maximum power in non-DUDe, can allow transmit power reduction via power control as the BS will be closely located in the case of DUDe. This finally results in reduction in interference and performance improvement at the network level [3]. Let us suppose that $\epsilon \in [0, 1]$ is the power control factor, full power control once $\epsilon = 1$, and no power control once $\epsilon = 0$.

3. Uplink SINR statistics

In this section, first of all a generic form of the CCDF of SINR is derived and then simple closed-form solutions for DUDe and non-DUDe are formulated. To derive the CCDF of SINR, association probabilities in uplink-downlink decoupled policy are required. In a two-tier HetNet, there are four possible association cases as given by [5]. In this paper we give only the final results.

- Case 1: Association probability for DL and UL with a macrocell is:

$$Pr\left[Case\ 1\right] = \frac{\lambda_m}{\lambda_m + \lambda_s} \tag{1}$$

- Case 2: Association probability for DL with a macrocell and UL with a small cell (femtocell or picocell) is:

$$Pr\left[Case\ 2\right] = \frac{\lambda_s}{\lambda_m + \lambda_s} - \frac{\lambda_s}{\lambda_m \left(\frac{P_m}{P_s}\right)^{\frac{2}{\alpha}} + \lambda_s} \tag{2}$$

- Case 3: Association probability for DL with a small cell and UL with a macrocell is:

$$Pr\left[Case\ 3\right] = 0. \tag{3}$$

- Case 4: Association probability for DL and UL with a femtocell or picocell is:

$$Pr\left[Case\ 4\right] = \frac{\lambda_s}{\lambda_m \left(\frac{P_m}{P_s}\right)^{2/\alpha} + \lambda_s} \tag{4}$$

In this paper, we limit our analysis specifically to those users who prefer decoupled access and are located in the DUDe area, as shown in Figure 1. To derive the CCDF of SINR, the probability density function (pdf) of statistical distance is required, and in this paper, we have used the already derived pdf of distance distributions for PPPs given in [6]. The pdf of R_d for the DUDe case is given as:

$$f_{R_d}\left(r_d\right) = \frac{2r_d\pi\lambda_s e^{-r_d^2\pi\lambda_s}\left(e^{-r_d^2\pi\lambda_m} - e^{r_d^2\pi\lambda_m\left(-\left(\frac{P_m}{P_s}\right)^{2/\alpha}\right)}\right)}{\frac{\lambda_s}{\lambda_m+\lambda_s} - \frac{\lambda_s}{\lambda_m\left(\frac{P_m}{P_s}\right)^{2/\alpha}+\lambda_s}} \tag{5}$$

where P_m and P_s are transmitted power levels of macrocells and small cells (femtocells or picocells), respectively. The pdf of R_{nd} for the non-DUDe case is:

$$f_{R_{nd}}\left(r_{nd}\right) = \frac{2r_{nd}\pi\lambda_m e^{-r_{nd}^2\pi\lambda_m}\left(e^{-r_{nd}^2\pi\lambda_s\left(\frac{P_s}{P_m}\right)^{2/\alpha}} - e^{-r_{nd}^2\pi\lambda_s}\right)}{\frac{\lambda_s}{\lambda_m+\lambda_s} - \frac{\lambda_s}{\lambda_m\left(\frac{P_m}{P_s}\right)^{2/\alpha}+\lambda_s}} \tag{6}$$

By using the above statistical distance distributions, the general form of the CCDF of SINR is calculated. The CCDF of SINR ($SINR_i$) in uplink is given as:

$$Pr\left[SINR_i > z\right] = Pr\left[\frac{P_u h_{r_i v} r_i^{(\epsilon-1)\alpha}}{\sum_{k=1}^{K} P_u r_{v,k}^{\epsilon\alpha} h_{r_k} r_k^{-\alpha}} + N_0 > z\right], \tag{7}$$

where K is the number of interferers in uplink and P_u is the transmitted power levels of UE. $r_{v,k}$ is the distance between the interferer and its serving cell. The r_k is the distance of the interferer from the target BS. By solving Eq. (7) for $h_{r_i v}$, we get:

$$Pr\left[SINR_i > z\right] = Pr\left[h_{r_i v} > \left(z\left(\sum_{k=1}^{K} r_{v,k}^{\epsilon\alpha} h_{r_k} r_k^{-\alpha} r_i^{(1-\epsilon)\alpha} + \frac{r_i^{(1-\epsilon)\alpha} N_0}{P_u}\right)\right)\right]. \tag{8}$$

Since $h_{r_i v}$ is an exponential random variable with unit mean and the association decision is based on average received signal power in UL, then, averaging over fading, Eq. (8) becomes:

$$Pr\left[SINR_i > z\right] = E\left[e^{-z\left(\sum_{k=1}^{K} r_{v,k}^{\epsilon\alpha} h_{r_k} r_k^{-\alpha} r_i^{(1-\epsilon)\alpha} + \frac{r_i^{(1-\epsilon)\alpha} N_0}{P_u}\right)}\right] \tag{9}$$

Summation of exponents can be written in product form and, assuming all r_k and h_{r_k} as independent, Eq. (9) can be conditioned over $K, ?r_i$ and we get:

$$Pr\left[SINR_i > z | K, r_i\right] = E\left[\prod_{k=1}^{K} e^{-\left(z r_{v,k}^{\epsilon\alpha} h_{r_k} r_k^{-\alpha} r_i^{(1-\epsilon)\alpha} + \frac{z r_i^{(1-\epsilon)\alpha} N_0}{P_u K}\right)}\right] \tag{10}$$

Since all K users experience similar conditions, Eq. (10) can be written as:

$$Pr\left[SINR_i > z | K, r_i\right] = \left[e^{-\frac{z r_i^{(1-\epsilon)\alpha} N_0}{P_u}}\right] E\left[e^{-z r_{v,k}^{\epsilon\alpha} h_{r_k} r_k^{-\alpha} r_i^{(1-\epsilon)\alpha}}\right]^K \tag{11}$$

Using the identity for Poisson K as $E[A^K] = e^{-E[K](1-A)}$ where $A = E\left[e^{-z r_{v,k}^{\epsilon\alpha} h_{r_k} r_k^{-\alpha} r_i^{(1-\epsilon)\alpha}}\right]$, conditioned on h_{r_k}:

$$Pr\left[SINR_i > z | K, r_i\right] = \left[e^{-\frac{z r_i^{(1-\epsilon)\alpha} N_0}{P_u}}\right] \times \left[e^{-E[K]\left[1 - E\left(e^{-z r_{v,k}^{\epsilon\alpha} h_{r_k} r_k^{-\alpha} r_i^{(1-\epsilon)\alpha}}\right)\right]}\right] \tag{12}$$

By solving Eq. (12) and removing condition on K, we get:

$$Pr\left[\left(SINR_i > z\right) | r_i\right] = \left[e^{-\frac{z r_i^{(1-\epsilon)\alpha} N_0}{P_u}}\right] e^{-E[K]\left(\int_c^b \frac{2r_k}{b^2} dr_k - \int_c^b e^{-z r_{v,k}^{\epsilon\alpha} E[h_{r_k}] r_k^{-\alpha} r_i^{(1-\epsilon)\alpha}} \frac{2r_k}{b^2} dr_k\right)} \tag{13}$$

where c is a random point for interferer location, which is outside the coverage area of a small cell. To meet OFDMA requirements, c has been chosen outside the coverage area of small cells in two-tier HetNets. Simplifying Eq. (13), we get:

$$Pr\left[(SINR_i > z)\,|r_i\right] = \left[e^{-\frac{zr_i^{(1-\epsilon)\alpha}N_0}{P_u}}\right] \times \left[e^{-\frac{E[K]}{b^2}\int_c^\infty \left(1-e^{-zr_{v,k}^{\epsilon\alpha}E[h_{r_k}]r_k^{-\alpha}r_i^{(1-\epsilon)\alpha}}\right)2r_k dr_k}\right], \tag{14}$$

where $E[h_k] = \Gamma\left(1+\frac{2}{\alpha}\right)$ and Γ is a gamma function. By removing the condition on r_i in Eq. (14), the general form of the uplink CCDF of SINR for DUDe and non-DUDe with power control and variable path loss factor can be found as:

$$Pr\left[SINR_i > z\right] = \int_0^\infty e^{-\frac{zr_i^{(1-\epsilon)\alpha}N_0}{P_u}} e^{-\frac{E[K]}{b^2}\int_c^\infty \left(1-e^{-zr_{v,k}^{\epsilon\alpha}\Gamma\left(1+\frac{2}{\alpha}\right)r_k^{-\alpha}r_i^{(1-\epsilon)\alpha}}\right)2r_k dr_k} f_{R_i}(r_i)dr_i \tag{15}$$

3.1. CCDF of SINR for DUDe

In this section, we derive the DUDe uplink CCDF of SINR for uniformly, nonuniformly, and interference-limited channels. In the first step, let us assume that interferers are uniformly distributed (c= 0) and $\alpha > 2$. By solving integration of Eq. (15) for r_k, we get:

$$Pr\left[SINR_d > z\right] = \int_0^\infty \left[e^{-\frac{zr_i^{(1-\epsilon)\alpha}N_0}{P_u}}\right] \left[e^{\frac{2E[K]}{b^{2\alpha}}r_{v,k}^{2\epsilon}r_i^{2(1-\epsilon)}z^{2/\alpha}\Gamma\left(1+\frac{2}{\alpha}\right)\Gamma\left(-\frac{2}{\alpha}\right)}\right] f_{R_i}(r_i)dr_i, \tag{16}$$

where $r_{v,k}$ is the distance between the interferer and its serving cell (macrocell, femtocell, or picocell) and as we know $E[K] = \lambda_I \pi b^2$. By using the pdf of R_d for DUDe given by Eq. (5) in Eq. (16), the general form of the CCDF of SINR with power control ϵ in uplink for DUDe is found as:

$$\begin{aligned} Pr\left[SINR_d > z\right] \;=\; & \int_0^\infty e^{\frac{-zr_d^\alpha N_0}{P_u}} e^{\frac{2\lambda_I \pi}{\alpha}r_{u,k}^{2\epsilon}r_i^{2(1-\epsilon)}z^{2/\alpha}\Gamma\left(1+\frac{2}{\alpha}\right)\Gamma\left(-\frac{2}{\alpha}\right)} \\ & \times \frac{2r_d\pi\lambda_s e^{-r_d^2\pi\lambda_s}\left(e^{-r_d^2\pi\lambda_m} - e^{r_d^2\pi\lambda_m\left(-\left(\frac{P_m}{P_s}\right)^{2/\alpha}\right)}\right)}{\frac{\lambda_s}{\lambda_m+\lambda_s} - \frac{\lambda_s}{\lambda_m\left(\frac{P_m}{P_s}\right)^{2/\alpha}+\lambda_s}} dr_d \end{aligned} \tag{17}$$

Eq. (17) cannot be solved for a general case of α. However, a closed-form solution for some plausible special cases, e.g., $\alpha = 4$ without ignoring noise and ϵ= 0, is given as:

$$r\left[SINR_d > z\right] = \left(\frac{\pi^{\frac{3}{2}}\left(\lambda_m+\lambda_s\right)\left(\lambda_s+\lambda_m\sqrt{\frac{P_m}{P_s}}\right)}{2\lambda_m\left(\sqrt{\frac{P_m}{P_s}}-1\right)\sqrt{\frac{N_0 z}{P_u}}}\right) \times \left(e^{\frac{\pi^2 P_u\left(\pi\sqrt{z}+2\right)^2\left(\lambda_m+\lambda_s\right)^2}{16N_0 z}} erfc\left(\frac{\pi\left(\pi\sqrt{z}+2\right)\left(\lambda_m+\lambda_s\right)}{4\sqrt{\frac{N_0 z}{P_u}}}\right)\right.$$
$$\left. P - \left(e^{\frac{\pi^2 P_u\left[\left(2\lambda_s+2\lambda_m\sqrt{\frac{P_m}{P_s}}\right)+\left(\pi\sqrt{z}\left(\lambda_m+\lambda_s\right)\right)\right]^2}{16N_0 z}}\right) \times erfc\left(\frac{\pi\left(\left[2\lambda_s+2\lambda_m\sqrt{\frac{P_m}{P_s}}\right]+\left[\pi\sqrt{z}\left(\lambda_m+\lambda_s\right)\right]\right)}{4\sqrt{\frac{N_0 z}{P_u}}}\right)\right) \quad (18)$$

Secondly, let $E\left[K\right]=\lambda_I\pi b^2$ and assume that interferers are nonuniformly distributed. This means that c is outside the coverage area of the target BS due to OFDMA. By solving integration of Eq. (15) for r_k and by using the pdf of R_d for DUDe given by Eq. (5), we get the following general form of DUDe with interferers outside the coverage area of the target BS and mobiles having power control in the uplink:

$$Pr\left[SINR_d > z\right] = \int_0^\infty e^{-\frac{z r_d^{(1-\epsilon)\alpha} N_0}{P_u}} \times e^{\frac{\lambda_I\pi}{\alpha}\left(\alpha c^2 - 2r_{u,k}^{2\epsilon} r_d^{2(1-\epsilon)} z^{2/\alpha}\Gamma\left(1+\frac{2}{\alpha}\right)\Gamma\left(-\frac{2}{\alpha},?c^{-\alpha} z\Gamma\left(1+\frac{2}{\alpha}\right) r_{v,k}^{\epsilon\alpha} r_d^{(1-\epsilon)\alpha}\right) - \Gamma\left(-\frac{2}{\alpha}\right)\right)}$$
$$\times \frac{2r_d\pi\lambda_s e^{-r_d^2\pi\lambda_s}\left(e^{-r_d^2\pi\lambda_m} - e^{r_d^2\pi\lambda_m\left(-\left(\frac{P_m}{P_s}\right)^{2/\alpha}\right)}\right)}{\frac{\lambda_s}{\lambda_m+\lambda_s} - \frac{\lambda_s}{\lambda_m\left(\frac{P_m}{P_s}\right)^{2/\alpha}+\lambda_s}} dr_d \quad (19)$$

For interference-limited channels (ignoring noise, $N_0 = 0$ with $c = 0$, and assuming worst-case scenario where no power control is applied, $\epsilon = 0$), the solution of Eq. (15) is as follows:

$$Pr\left[SINR_d > z\right] = \int_0^\infty e^{-\frac{E[K]}{b^2}\int_0^\infty\left(1-e^{-z\Gamma\left(1+\frac{2}{\alpha}\right)r_k^{-\alpha}r_d^{\alpha}}\right)2r_k dr_k} \times f_{R_d}(r_d) \quad (20)$$

By inserting the pdf of R_d for DUDe given by Eq. (5) and $E\left[K\right]=\lambda_I\pi b^2$, the solution of (20) after solving the integration $\int_0^\infty\left(1-e^{-z\Gamma\left(1+\frac{2}{\alpha}\right)r_k^{-\alpha}r_d^{\alpha}}\right)2r_k dr_k = -2\frac{\left(z\Gamma\left(1+\frac{2}{\alpha}\right)r_k^{-\alpha}r_d^{\alpha}\right)^{2/\alpha}\Gamma\left(-\frac{2}{\alpha}\right)}{\alpha}$ is as follows:

$$Pr\left[SINR_d > z\right] = \int_0^\infty e^{2\lambda_I\pi\frac{\left(z\Gamma\left(1+\frac{2}{\alpha}\right)r_k^{-\alpha}r_d^{\alpha}\right)^{\frac{2}{\alpha}}\Gamma\left(-\frac{2}{\alpha}\right)}{\alpha}} \times \frac{2r_d\pi\lambda_s e^{-r_d^2\pi\lambda_s}\left(e^{-r_d^2\pi\lambda_m} - e^{r_d^2\pi\lambda_m\left(-\left(\frac{P_m}{P_s}\right)^{2/\alpha}\right)}\right)}{\frac{\lambda_s}{\lambda_m+\lambda_s} - \frac{\lambda_s}{\lambda_m\left(\frac{P_m}{P_s}\right)^{2/\alpha}+\lambda_s}} dr_d \quad (21)$$

Let $A = \frac{\lambda_s}{\lambda_m+\lambda_s} - \frac{\lambda_s}{\lambda_m\left(\frac{P_m}{P_s}\right)^{2/\alpha}+\lambda_s}$, $B = \frac{2\lambda_I\pi\left(z\Gamma\left(1+\frac{2}{\alpha}\right)\right)^{2/\alpha}\Gamma\left(-\frac{2}{\alpha}\right)}{\alpha}$, and $\lambda_I = \lambda_m + \lambda_s$. Simplifying Eq. (2), we get:

$$Pr\left[SINR_d > z\right] = \int_0^\infty \frac{2\pi\lambda_s r_d}{A} e^{r_d^2(B-\pi(\lambda_m+\lambda_s))} - e^{r_d^2\left(B-\pi\left(\lambda_m+\lambda_s\left(\frac{P_m}{P_s}\right)^{2/\alpha}\right)\right)} dr_d \quad (22)$$

By solving integration of Eq. (22) into parts for r_d, the DUDe CCDF of SINR closed-form solution for a general case of α, not previously available in the literature, is as follows:

$$Pr\left[SINR_d > z\right] = \frac{\alpha^2\left(\lambda_s + \lambda_m\left(\frac{P_m}{P_s}\right)^{2/\alpha}\right)}{\left(\alpha + 2\pi\csc\left(\frac{2\pi}{\alpha}\right)z^{2/\alpha}\right)} \times \frac{1}{\left[\alpha\left(\lambda_s + \lambda_m\left(\frac{P_m}{P_s}\right)^{2/\alpha}\right) + 2\pi\csc\left(\frac{2\pi}{\alpha}\right)(\lambda_m + \lambda_s)z^{2/\alpha}\right]} \tag{23}$$

3.2. CCDF of SINR for non-DUDe

In this section, we derive the non-DUDe uplink CCDF of SINR for uniformly, nonuniformly, and interference-limited channels. The procedure used to find the DUDe CCDF of SINR can also be used to find the non-DUDe CCDF of SINR. By using the pdf of R_{nd} for non-DUDe given by Eq. (6) in Eq. (15), the closed-form solution of the CCDF of SINR for non-DUDe for $\alpha = 4$ with noise and uniformly distributed interferers is:

$$\begin{aligned} Pr\left[SINR_{nd} > z\right] \;=\; & -\left(\frac{\pi^{3/2}(\lambda_m + \lambda_s)\left(\lambda_s + \lambda_m\sqrt{\frac{P_m}{P_s}}\right)}{2\lambda_s\left(\sqrt{\frac{P_m}{P_s}} - 1\right)\sqrt{\frac{N_0 z}{P_u}}}\right) \\ & \times\left(e^{\frac{\pi^2 P_u\left(\pi\sqrt{z}+2\right)^2(\lambda_m+\lambda_s)^2}{16N_0 z}} erfc\left(\frac{\pi\left(\pi\sqrt{z}+2\right)(\lambda_m+\lambda_s)}{4\sqrt{\frac{N_0 z}{P_u}}}\right)\right. \\ & -\left(e^{\frac{\pi^2 P_u\left(2\lambda_m + 2\lambda_s\sqrt{\frac{P_s}{P_m}} + \pi\lambda_m\sqrt{z} + \pi\lambda_s\sqrt{z}\right)^2}{16N_0 z}}\right) \\ & \left.\times erfc\left(\frac{\pi\left(2\lambda_m + 2\lambda_s\sqrt{\frac{P_s}{P_m}} + \pi\lambda_m\sqrt{z} + \pi\lambda_s\sqrt{z}\right)}{4\sqrt{\frac{N_0 z}{P_u}}})\right)\right) \end{aligned} \tag{24}$$

By solving integration of Eq. (15) for r_k and by using the pdf of R_{nd} for non-DUDe given by Eq. (6), we get the general form of the non-DUDe CCDF of SINR with interferers nonuniformly distributed and having power control in uplink as:

$$\begin{aligned} Pr\left[SINR_{nd} > z\right] \;=\; & \int_0^\infty e^{-\frac{z r_{nd}^{(1-\epsilon)\alpha} N_0}{P_u}} \times e^{\frac{\lambda_I \pi}{\alpha}\left(\alpha c^2 - \left[2r_{u,k}^{2\epsilon} r_{nd}^{2(1-\epsilon)} z^{2/\alpha}\Gamma\left(1+\frac{2}{\alpha}\right)\Gamma\left(-\frac{2}{\alpha}, c^{-\alpha} z\Gamma\left(1+\frac{2}{\alpha}\right) r_{v,k}^{\epsilon\alpha} r_{nd}^{(1-\epsilon)\alpha}\right) - \Gamma\left(-\frac{2}{\alpha}\right)\right]\right)} \\ & \times \frac{2r_{nd}\pi\lambda_m e^{-r_{nd}^2\pi\lambda_m}\left(e^{-r_{nd}^2\pi\lambda_s\left(\frac{P_s}{P_m}\right)^{2/\alpha}} - e^{-r_{nd}^2\pi\lambda_s}\right)}{\frac{\lambda_s}{\lambda_m+\lambda_s} - \frac{\lambda_s}{\lambda_m\left(\frac{P_m}{P_s}\right)^{2/\alpha}+\lambda_s}} dr_{nd}, \end{aligned} \tag{25}$$

where $r_{v,k}$ is the distance between the interferer and its serving macrocell. For interference-limited channels (ignoring noise, $N_0 = 0$ with $c = 0$, and assuming worst-case scenario where no power control is applied, $\epsilon = 0$), the solution of Eq. (15) is as follows:

$$Pr\left[SINR_{nd} > z\right] = \int_0^\infty e^{-\frac{E[K]}{b^2}\int_0^\infty\left(1 - e^{-z\Gamma\left(1+\frac{2}{\alpha}\right)r_k^{-\alpha} r_d^{\alpha}}\right)2r_k dr_k} \times f_{R_{nd}}(r_{nd}). \tag{26}$$

By inserting the pdf of R_{nd} for non-DUDe given by Eq. (6) and $E[K] = \lambda_I \pi b^2$, the solution of Eq. (26) after solving the integration

$$\int_0^\infty \left(1 - e^{-z\Gamma\left(1+\frac{2}{\alpha}\right) r_k^{-\alpha} r_d^{\alpha}}\right) 2r_k dr_k = -\frac{\left(z\Gamma\left(1+\frac{2}{\alpha}\right) r_k^{-\alpha} r_d^{\alpha}\right)^{2/\alpha} \Gamma\left(-\frac{2}{\alpha}\right)}{\alpha}$$

is as follows:

$$\begin{aligned} Pr\left[SINR_{nd} > z\right] &= \int_0^\infty e^{2\lambda_I \pi} \frac{\left(z\Gamma\left(1+\frac{2}{\alpha}\right) r_k^{-\alpha} r_d^{\alpha}\right)^{2/\alpha} \Gamma\left(-\frac{2}{\alpha}\right)}{\alpha} \\ &\times \frac{2r_{nd}\pi\lambda_m e^{-r_{nd}^2 \pi \lambda_m} \left(e^{-r_{nd}^2 \pi \lambda_s \left(\frac{P_s}{P_m}\right)^{2/\alpha}} - e^{-r_{nd}^2 \pi \lambda_s}\right)}{\frac{\lambda_s}{\lambda_m+\lambda_s} - \frac{\lambda_s}{\lambda_m \left(\frac{P_m}{P_s}\right)^{2/\alpha} + \lambda_s}} dr_{nd} \end{aligned} \tag{27}$$

Let $A = \frac{\lambda_s}{\lambda_m+\lambda_s} - \frac{\lambda_s}{\lambda_m \left(\frac{P_m}{P_s}\right)^{2/\alpha} + \lambda_s}$, $B = \frac{2\lambda_I \pi \left(z\Gamma\left(1+\frac{2}{\alpha}\right)\right)^{2/\alpha} \Gamma\left(-\frac{2}{\alpha}\right)}{\alpha}$, and $\lambda_I = \lambda_m + \lambda_s$. Simplifying Eq. (27), we get:

$$Pr\left[SINR_{nd} > z\right] = \int_0^\infty \frac{2\pi\lambda_m r_{nd}}{A} e^{r_{nd}^2 \left(B - \pi\left(\lambda_m + \lambda_s \left(\frac{P_s}{P_m}\right)^{2/\alpha}\right)\right)} - e^{r_{nd}^2 (B - \pi(\lambda_m+\lambda_s))} dr_{nd} \tag{28}$$

By solving integration of Eq. (28) into parts for r_{nd}, the closed-form solution for a general case of α is as follows:

$$\begin{aligned} tPr\left[SINR_{nd} > z\right] &= -\frac{\alpha\left(\lambda_m + \lambda_s\right)\left(\lambda_s + \lambda_m \left(\frac{P_m}{P_s}\right)^{\frac{2}{\alpha}}\right)}{\lambda_s \left(\left(\frac{P_m}{P_s}\right)^{\frac{2}{\alpha}} - 1\right)} \\ &\times \left(\frac{1}{\left(\lambda_m + \lambda_s\right)\left(\alpha + 2\pi \csc\left(\frac{2\pi}{\alpha}\right) z^{\frac{2}{\alpha}}\right)} - \frac{1}{\alpha\left(\lambda_m + \lambda_s \left(\frac{P_m}{P_s}\right)^{\frac{2}{\alpha}}\right) + 2\pi \csc\left(\frac{2\pi}{\alpha}\right)\left(\lambda_m + \lambda_s\right) z^{\frac{2}{\alpha}}}\right). \end{aligned} \tag{29}$$

Eq. (29) gives the non-DUDe CCDF of SINR for interference-limited channels for a general case of α. This general form of non-DUDe CCDF of SINR for variable path loss factor was not previously available in the literature. Using the desired results of this section, we find the average throughput for DUDe and non-DUDe in the next section.

4. Uplink average throughput

The normalized throughput η_i (bits/s/Hz), as per [5], is defined as:

$$\eta_i = \frac{1}{N_i}\left[log_2(1+z) Pr\left[SINR_i > z\right]\right] \tag{30}$$

where $i = d$ for DUDe, $i = nd$ for non-DUDe, z is the SINR threshold, and $Pr\left[SINR_i > z\right]$ is the probability that user SINR is greater than threshold z, which is calculated by using Eqs. (18) and (24). The average

number of associated devices is represented as $N_i = \lambda_u \frac{A_d}{\lambda_v}$ and A_d is the association probability as given by Eq. (2). The decoupled association probability, A_d, is the same for both DUDe and non-DUDe as we are only considering those users for analysis that can be decoupled in DL-UL. The closed-form solution for DUDe average throughput without ignoring noise can be found by using Eqs. (18) and (30) as follows:

$$\eta_d = \left(\frac{1}{\frac{\lambda_u}{\lambda_s}\left(\frac{\lambda_s}{\lambda_m+\lambda_s} - \frac{\lambda_s}{\lambda_m\left(\frac{P_m}{P_s}\right)^{\frac{2}{\alpha}}+\lambda_s} \right)} log_2\left(1+z\right) \right) \times \left(\frac{\pi^{\frac{3}{2}}\left(\lambda_m+\lambda_s\right)\left(\lambda_s+\lambda_m\sqrt{\frac{P_m}{P_s}}\right)}{2\lambda_m\left(\sqrt{\frac{P_m}{P_s}}-1\right)\sqrt{\frac{N_0 z}{P_u}}} \right)$$
$$\times \left(e^{\frac{\pi^2 P_u(\pi\sqrt{z}+2)^2(\lambda_m+\lambda_s)^2}{16N_0 z}} erfc\left(\frac{\pi\left(\pi\sqrt{z}+2\right)\left(\lambda_m+\lambda_s\right)}{4\sqrt{\frac{N_0 z}{P_u}}} \right) - \left(e^{\frac{\pi^2 P_u\left[\left(2\lambda_s+2\lambda_m\sqrt{\frac{P_m}{P_s}}\right)+\left(\pi\sqrt{z}(\lambda_m+\lambda_s)\right)\right]^2}{16N_0 z}} \right) \right.$$
$$\left. \times erfc\left(\frac{\pi\left[\left(2\lambda_s+2\lambda_m\sqrt{\frac{P_m}{P_s}}\right)+\left(\pi\sqrt{z}\left(\lambda_m+\lambda_s\right)\right)\right]}{4\sqrt{\frac{N_0 z}{P_u}}} \right) \right). \tag{31}$$

For non-DUDe, the closed-form solution for average throughput by using Eqs. (24) and (30), without ignoring noise, is:

$$\eta_{nd} = -\left(\frac{1}{\frac{\lambda_u}{\lambda_m}\left(\frac{\lambda_s}{\lambda_m+\lambda_s} - \frac{\lambda_s}{\lambda_m\left(\frac{P_m}{P_s}\right)^{2/\alpha}+\lambda_s} \right)} log_2(1+z) \right) \times \left(\frac{\pi^{3/2}(\lambda_m+\lambda_s)\left(\lambda_s+\lambda_m\sqrt{\frac{P_m}{P_s}}\right)}{2\lambda_s\left(\sqrt{\frac{P_m}{P_s}}-1\right)\sqrt{\frac{N_0 z}{P_u}}} \right)$$
$$\times \left(e^{\frac{\pi^2 P_u(\pi\sqrt{z}+2)^2(\lambda_m+\lambda_s)^2}{16N_0 z}} erfc\left(\frac{\pi\left(\pi\sqrt{z}+2\right)\left(\lambda_m+\lambda_s\right)}{4\sqrt{\frac{N_0 z}{P_u}}} \right) - \left(e^{\frac{\pi^2 P_u\left(2\lambda_m+2\lambda_s\sqrt{\frac{P_s}{P_m}}+\pi\lambda_m\sqrt{z}+\pi\lambda_s\sqrt{z}\right)^2}{16N_0 z}} \right) \right.$$
$$\left. \times erfc\left(\frac{\pi\left(2\lambda_m+2\lambda_s\sqrt{\frac{P_s}{P_m}}+\pi\lambda_m\sqrt{z}+\pi\lambda_s\sqrt{z}\right)}{4\sqrt{\frac{N_0 z}{P_u}}} \right) \right) \tag{32}$$

5. Numerical results

The proposed system model and the corresponding analytical results are validated by MATLAB simulations in two-tier HetNet settings with P_m = 46 dBm for macrocells; P_s = 20 dBm for femtocells or picocells; P_u = 20 dBm; $\lambda_s = 5\lambda_m$; and $\alpha = 4$. Users, macrocells, picocells, and femtocells are distributed through PPPs and analysis is performed for a target user located at the origin. Initially, user associations with BSs are established to categorize them as per their types, CoA or DUDe. Later on, simulation and analytical results for DUDe users are plotted for the CCDF of SINR and average throughput for varying SINR thresholds and HetNet densities. For comparison purposes, no power control has been used to exhibit the lower bound of DUDe gains over non-DUDe. Figures 2a and 2b show association probabilities for two-tier HetNets with decoupling permissibility for varying network densities and power levels, respectively. Results show that with an increase of network densification, more users prefer decoupled access. However, not all network users choose decoupled access; rather, their UL-DL remains associated with the same BS. Most of the network users maintain coupled associations once densities of small cells are less as compared to macrocells. However, this coupled association preference reduces with increase of HetNet densification and more users start using UL-DL decoupled association

with two different BSs. However, there is an upper bound on this increase and, at a certain level, users start associating their UL and DL with the same small cell due to their availability in the close vicinity. In the case of femto to macro power ratio increase, decoupling association probability decreases and users start associating their UL-DL with the same small cell.

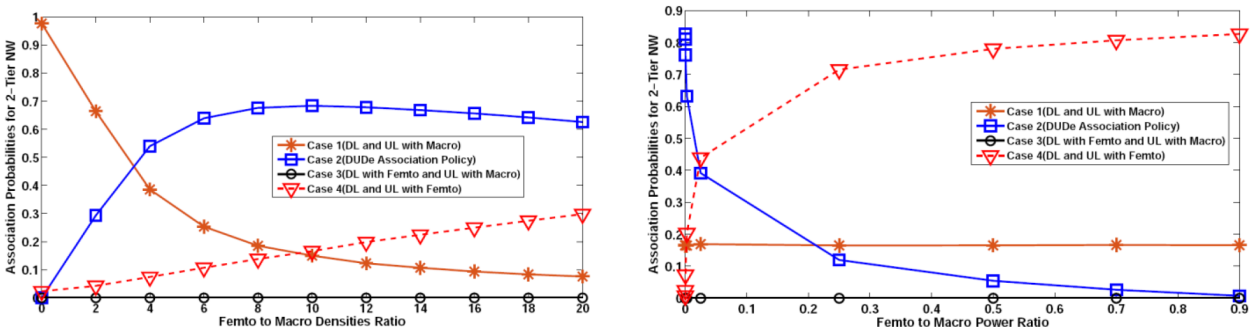

Figure 2. Two-tier association probabilities: a) densities effect, b) BS power effect.

Figure 3 shows simulation and analytical results for the CCDF of SINR and average throughput. In each graph, analytical and simulation results are plotted for varying QoS indicators. Black solid lines in Figures 3a and 3b show the CCDF of SINR and average throughput analytical results, respectively, for users with decoupled association. Stars on these lines show the simulation results for decoupled users. Similarly, results for non-DUDe users are also shown in Figures 3a and 3b with boxes over the line. The lines with circles in Figures 3a and 3b show the advantage of DUDe association over non-DUDe association. In Figure 3a, at SINR threshold = –10, 0, 10, 15, 30 dBs, the CCDF of SINR for DUDe is approximately 3, 6, 11.3, 14.12, and 18.53 times higher than non-DUDe, respectively. In Figure 3b, due to logarithmic terms in Eq. (12) and (13), initially the average throughput increases, and then at a certain SINR threshold, it starts decreasing. In Figure 3b, at SINR threshold = –10, 0, 10, 15, 30 dBs, average throughput is approximately 15, 31, 56.6, 70, and 92.6 times higher than non-DUDe, respectively. Numerical results clearly show that as the SINR threshold is increased, DUDe's advantage over non-DUDe increases because non-DUDe users have lower SINR as compared to DUDe users. These results also show that decoupled association gives significant advantages over non-DUDe and not all network users prefer decoupled access.

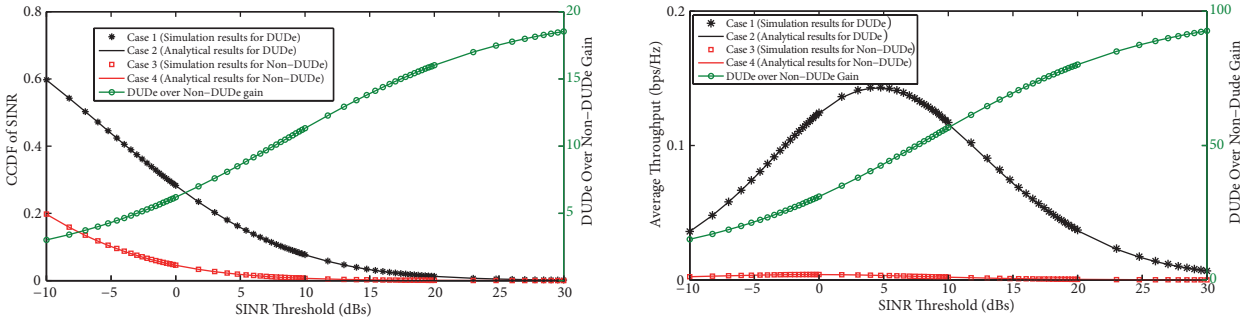

Figure 3. Performance graphs: a) CCDF of SINR, b) average throughput.

Effects of network densities on the CCDF of SINR and average throughput have also been analyzed to relate network performance to the degree of HetNet densification to facilitate the design of efficient cellular networks where QoS objectives can be assured in advance. Figures 4a and 4b show simulation and analytical results for the CCDF of SINR and average throughput at SINR threshold = 0 dBs, respectively. In these

graphs, HetNet densification has been varied to present insights about the performance of decoupled users. It is clearly evident from these results that by increasing small cell densities, the performance gain of decoupled users is increased. However, in the case of non-DUDe, an increase in network densification does not affect the performance of users. With the increase of femtocell to macrocell densities, the CCDF of SINR increases for DUDe, whereas it remains almost constant for non-DUDe. Hence, density effect is more prominent in DUDe than non-DUDe. Consequently, our analytical solution can be used to find the practical situations to determine lower and upper bounds of HetNet densification with decoupled access to assure QoS requirements to users that are underprivileged in DLRP-based user associations.

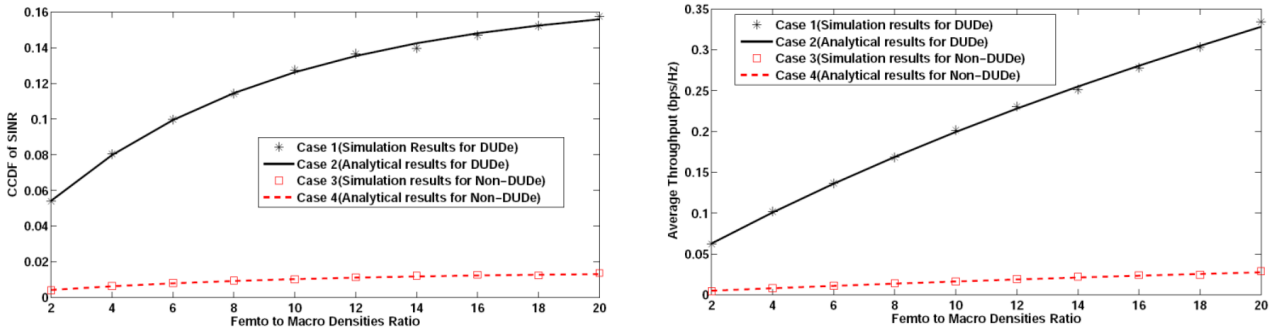

Figure 4. HetNet densification effect: a) CCDF of SINR, b) average throughput.

Effects of BS power levels on the CCDF of SINR and average throughput have also been analyzed to exhibit the DUDe region's relation with BS power levels. Figures 5a and 5b show simulation and analytical results for the CCDF of SINR and average throughput, respectively (at SINR threshold = 0 dBs, $P_m = 46$ dBm, and $\lambda_s = 5\lambda_m$). In these graphs, power levels of small cells have been varied while keeping the power levels of macrocells constant to present the effects on user performance. It is clearly evident from these graphs that DUDe user CCDF of SINR decreases whereas non-DUDe user CCDF of SINR increases as more users start preferring coupled access. With the increase of femtocell to macrocell power levels, average throughput and decoupled association probability of both DUDe and non-DUDe users rise due to increase of small cell power levels. It is also worth mentioning that the simulation and analytical results of Figures 3–5 completely match each other. This corroboration confirms the correctness of our mathematical model for use by network operators and designers. Figure 6 gives the effect of noise on the analytical model. From the results, it is evident that ignoring noise in the analytical model may lead to inaccurate performance metrics.

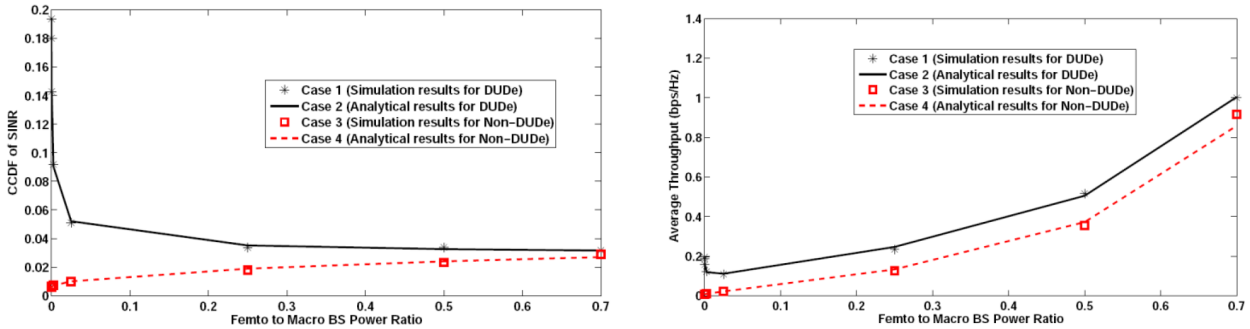

Figure 5. HetNet BS power effect: a) CCDF of SINR, b) average throughput.

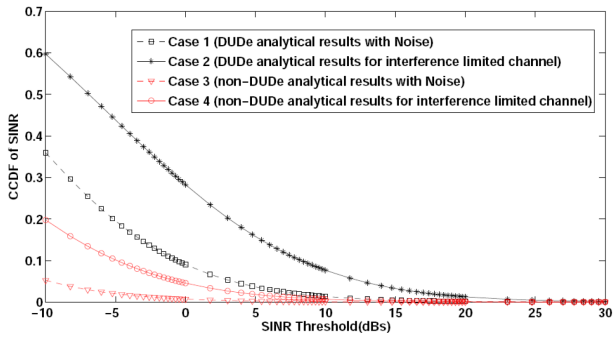

Figure 6. Effect of noise on analytical model.

6. Practical HetNet architecture for decoupled access

In view of the presented analytical model, decoupled association requires some changes to the network architecture to allow ongoing coupled and new decoupled associations. The architecture has to meet high user mobility, traffic latency, back-haul capacity, and network reliability requirements. In this paper, we propose a new network architecture for decoupled access by utilizing the architectures of 3GPP and Smiljkvikj et al. [6] as the baseline. In order to limit changes to the existing network, we propose that network access policy may be changed only for DUDe devices instead of making changes to all network users. Figure 7 gives the practical HetNet architecture with coupled and decoupled access policy. Two separate call setup policies, one for DUDe users and another for the remaining CoA users, can be defined and chosen during the call setup procedure considering user mobility status and back-haul load conditions. High mobility users may not use the decoupling policy as it will increase complex UL-DL handovers and resource management overheads at network

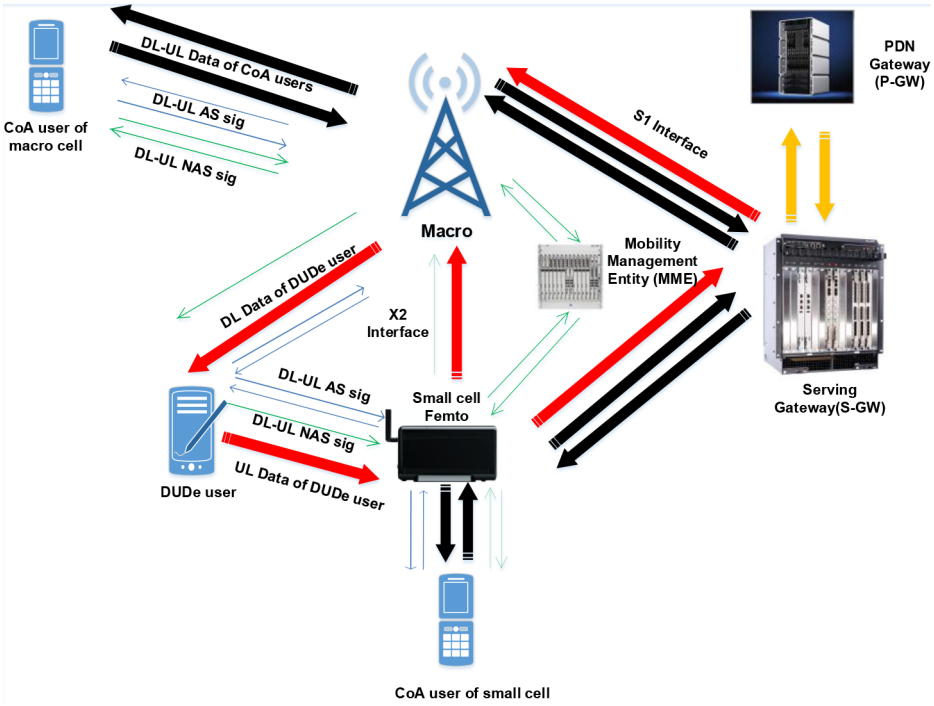

Figure 7. Proposed practical HetNet with decoupled access.

levels, counterbalancing the decoupling advantages. In the LTE network, the *X2* interface is used for handovers and interference coordination between two network nodes. This *X2* interface can be used to route UL traffic, access stratum (AS, layer 1–2, radio resource control signaling between user equipment and BS), and nonaccess stratum (NAS, control signaling exchanged between user equipment and core network) control signaling between two nodes for reassembly. However, as *X2* interface traffic loads are mostly 5% of the S1 interface, the back-haul load capacity may limit network performance. To address this limitation, the core network can be used to route UL traffic and control signaling for decoupled users, which may also be limited by load capacities. To address this aspect, it is important that the UL traffic of only DUDe devices may be routed through the *X2* interface or core network and path selection, i.e. the *X2* or core network may be decided by the BS at the time of call setup. Thus, UL traffic and NAS control signals of decoupled users are routed through the *X2* interface or core network depending upon back-haul load conditions. The traffic and control signaling of the remaining CoA network users can follow the existing traffic routing policy in which both UL and DL traffic is routed through the same BS. The algorithm for the proposed cell association policy is given in Algorithm 1. According to our proposed algorithm, a user can select from the two user association options, i.e. coupled or decoupled, to limit the network infrastructure changes, which is different from existing association algorithms. The user association type decision is made on the basis of location, access type benefits, BS densities, HetNet tiers, back-haul status, mobility conditions, and BS power levels. At present, these factors are not considered during the cell association process.

7. Conclusions

DUDe for HetNet is a recent concept to solve the weaknesses of existing cell associations. Previously proposed decoupled models are theoretical without giving practical realization. This paper proposes a new practical hybrid scheme in which coupled or decoupled cell association can be selected depending upon user location and its advantages. This method is practical in nature and can be employed in 5G HetNets to achieve fairness, cell load balancing, and performance improvements. We have presented the UL analysis framework for those users who are mainly affected by decoupling instead of earlier attempts where all network users are assumed to utilize decoupled access without considering its practicability. By using this model, simple analytical closed-form solutions without ignoring noise have been derived, not previously available in the literature. The derived distributions relate network performance to HetNet densities to assure QoS to users who are underprivileged in DLRP-based user associations. Analysis shows that as HetNet densification is increased, more users prefer decoupled access. Finally, practical network architecture for decoupled access has been proposed. For our proposed hybrid access, we have used user location to determine the access type as decoupled or coupled. Constraints other than location, such as load balancing or QoS, can also be incorporated in the user association policy to further improve the performance of network users. Moreover, decoupled access can also be used in combination with cell range extension and dual connectivity to further improve load balancing and user throughput. This is certainly a key future research direction to further improve fairness, cell load balancing, and performance of network users.

Algorithm 1 Algorithm for proposed cell association policy.

HetNet settings

Density of macrocells = λ_m, density of small cells = λ_s, and density of users = λ_u
Macrocell tx power = P_m, small cell tx power = P_s, and user equipment tx power = P_u
Let target user be denoted as *UE*, no. of macrocells = m, and no. of small cells = s
Let distance between *UE* and cell under consideration = r_i and SINR threshold = z

Downlink cell association

for all m and s Cells
Compute $Pwr_{DLRP,m} = P_m \parallel r_m \parallel^{\alpha}$ received by UE for each macrocell
Compute $Pwr_{DLRP,s} = P_s \parallel r_s \parallel^{\alpha}$ received by UE for each small cell
end for
UE evaluates power reports of all cells (s,m) and selects the cell with max DLRP
if Selected DL Cell = m then DL with macrocell
else DL with small cell
endif

Uplink cell association

for all m and s Cells
Compute $Pwr_{UL,m} = P_u \parallel r_m \parallel^{\alpha}$ received by macrocells from UE
Compute $Pwr_{UL,s} = P_u \parallel r_s \parallel^{\alpha}$ received by small cell from UE
end for
UE receives power reports from all cells (s,m) and selects the cell with max uplink power based on minimum path loss
if Selected UL Cell = m then UL with macrocell
else UL with small cell
endif

Association cases

if DL-UL with macrocell or DL-UL with small cell
then UE association is CoA (use existing cell association policy)
else UE is DUDe user and located in DUDe region
endif

Performance metrics for DUDe users

Compute SINR by using Eq. (7) and average throughput by using Eq. (30)

Call setup for DUDe users

if *SINR* > z
if UE mobility status = low, decouple UL and DL
UE gets *X2* and core back-haul load status
if *X2* load conditions = low
Route UL traffic and NAS control signals through *X2*
else Route traffic and control signals through core NW
endif
else Use coupled association (CoA) endif
endif

References

[1] Gavrilovska L, Rakovic V, Atanasovski V. Visions towards 5G: technical requirements and potential enablers. Wireless Pers Commun 2016; 87: 731-757.

[2] Boccardi F, Heath RW, Lozano A, Marzetta TL, Popovski P. Five disruptive technology directions for 5G. IEEE Commun Mag 2014; 52: 74-80.

[3] Boccardi F, Andrews JG, Elshaer H, Dohler M, Parkvall S, Popovski P, Singh S. Why to decouple the uplink and downlink in cellular networks and how to do it. IEEE Commun Mag 2016; 54: 110-117.

[4] Jo HS, Sang YJ, Xia P, Andrews JG. Heterogeneous cellular networks with flexible cell association: a comprehensive downlink SINR analysis. IEEE T Wirel Commun 2012; 11: 3484-3495.

[5] Smiljkovikj K, Popovski P, Gavrilovska L. Analysis of the decoupled access for downlink and uplink in wireless heterogeneous networks. IEEE Wirel Commun Lett 2015; 4: 173-176.

[6] Smiljkovikj K, Popovski P, Gavrilovska L. Capacity analysis of decoupled downlink and uplink access in 5G heterogeneous systems. arXiv: 1410.7270.

[7] Singh S, Zhang X, Andrews JG. Joint rate and SINR coverage analysis for decoupled uplink-downlink biased cell associations in HetNets. IEEE T Wirel Commun 2015; 14: 5360-5373.

[8] Elbamby MS, Bennis M, Latva-Aho M. UL/DL decoupled user association in dynamic TDD small cell networks. In: International Symposium on Wireless Communication Systems; 25–28 August 2015; Brussels, Belgium. New York, NY, USA: IEEE. pp. 456-460.

[9] Singh S, Zhang X, Andrew JG. Uplink rate distribution in heterogeneous cellular networks with power control and load balancing. In: IEEE International Conference on Communication Workshop; 8–12 June 2015; London, UK. New York, NY, USA: IEEE. pp. 1275-1280.

[10] Chiu SN, Stoyan D, Kendall WS, Mecke J. Stochastic Geometry and Its Applications. New York, NY, USA: Wiley, 2013.

[11] Sui X, Zhao Z, Li R, Zhang H. Energy efficiency analysis of heterogeneous cellular networks with downlink and uplink decoupling. In: Global Communications Conference; 6–10 December 2015; San Diego, CA, USA. New York, NY, USA: IEEE. pp. 1-7.

[12] Dhillon HS, Andrews JG. Downlink rate distribution in heterogeneous cellular networks under generalized cell selection. IEEE Wirel Commun Lett 2014; 3: 42-45.

[13] Baccelli F, Blaszczyszyn B. Stochastic Geometry and Wireless Networks. Foundations and Trends in Networking. Hanover, MA, USA: Now Publishers, 2010.

[14] Lin Y, Bao W, Yu W, Linag B. Optimizing user association and spectrum allocation in HetNets: a utility perspective. IEEE J Sel Area Comm 2015; 33: 1025-1039.

[15] Novlan TD, Dhillon HS, Andrews JG. Analytical modeling of uplink cellular networks. IEEE T Wirel Commun 2013; 12: 2669-2679.

[16] Damnjanovic A, Montojo J, Wei Y, Ji T, Luo T, Vajapeyam M, Yoo T, Song O, Malladi D. A survey on 3GPP heterogeneous networks. IEEE Wirel Commun 2011; 18: 10-21.